

Dalitz plot analyses with $B \rightarrow Dhh$ decays at LHCb

Wenbin Qian^{*†}

Laboratoire d'Annecy-le-Vieux de Physique des Particules

E-mail: Wenbin.Qian@cern.ch

Decays of b -hadrons to three-body final states including an open-charmed meson provide a rich laboratory to constrain the unitarity triangle and search for new physics. Recent measurements in this sector are presented in these proceedings, including measurements of the properties of the newly observed $D_{(s)}$ excited states, study of $f_0(500)$ and $f_0(980)$ substructures and final-state interactions in $B \rightarrow D\rho$ system.

The European Physical Society Conference on High Energy Physics
22–29 July 2015
Vienna, Austria

^{*}Speaker.

[†]On behalf of the LHCb collaboration

1. Introduction

Decays of b -hadrons to three-body final states including an open-charmed meson provide a rich laboratory to constrain the unitarity triangle. The Dalitz plot analysis of $B^0 \rightarrow \bar{D}^0 K^+ \pi^-$ can be used to constrain the CKM angle γ [1] while a time-dependent Dalitz plot analysis of the $B^0 \rightarrow \bar{D}^0 \pi^+ \pi^-$ ($B_s^0 \rightarrow \bar{D}^0 K^+ K^-$) decay gives sensitivity to the CKM angle $\beta_{(s)}$ (and γ for the B_s^0 decay) [2]. The large amount of data collected by the LHCb experiment offers an ideal place to study excited $D_{(s)}$ meson spectroscopy and structures of light mesons decaying to $\pi^+ \pi^-$ and $K^+ K^-$ final states [3]. The $B \rightarrow Dhh$ decays have been extensively studied by the LHCb experiment using the 3 fb^{-1} data collected during 2011 and 2012. The latest Dalitz plot analysis results are described in these proceedings, including those from the $B^0 \rightarrow \bar{D}^0 \pi^+ \pi^-$ [4], $B^0 \rightarrow \bar{D}^0 K^+ \pi^-$ [5], $B^- \rightarrow D^+ K^- \pi^-$ [6] and $B_s^0 \rightarrow \bar{D}^0 K^- \pi^+$ [7] decays.

2. Dalitz plot analysis

Similar Dalitz plot analysis strategies are applied on all the decay channels considered. An unbinned extended maximum likelihood fit is performed to the Dalitz plot distribution.

The signal probability density function (PDF) on Dalitz plot (\vec{x}) , $f_s(\vec{x}; \theta_s)$, is described by

$$\frac{M(\vec{x}; \theta_s) \varepsilon(\vec{x})}{\int M(\vec{x}; \theta_s) \varepsilon(\vec{x}) d\vec{x}} \quad (2.1)$$

The decay amplitude, $M(\vec{x}; \theta)$, is modeled by the isobar formalism where contributions from quasi-two-body decays are summed coherently. For the $\pi^+ \pi^-$ S-wave, the K-matrix formalism is also used. The fit parameters, θ_s , include complex coefficients and resonant parameters like masses and widths. The efficiency variation over the Dalitz plot, $\varepsilon(\vec{x})$, is obtained from Monte Carlo with data-driven method to correct for the difference between data and Monte Carlo. It is either modeled explicitly using polynomial functions or described by the spline technique.

The background PDF, $f_b(\vec{x})$, includes contributions from combinatorial background, mis-identified background and partially reconstructed background. Mis-identified and partially reconstructed background contributions are either suppressed to negligible level or modeled explicitly using Dalitz models obtained from previous analyses. The combinatorial background contribution is modeled using that of the sideband.

The unbinned likelihood function is then defined by

$$\mathcal{L} = \frac{e^{-(v_s+v_b)} (v_s + v_b)^N}{N!} \prod_{i=1}^N \left[\frac{v_s}{v_s + v_b} f_s(\vec{x}_i; \theta_s) + \frac{v_b}{v_s + v_b} f_b(\vec{x}_i) \right], \quad (2.2)$$

where the value N is the total number of reconstructed candidates in the signal region. The number of signal and background events, v_s and v_b , are floated and constrained by the yields determined from invariant mass fit of b -hadron candidates.

To improve sensitivity and reduce systematic uncertainties due to background, optimized selection criteria are applied to achieve clean environment for Dalitz plot analysis. The invariant mass distribution of $B^0 \rightarrow \bar{D}^0 \pi^+ \pi^-$ candidates is shown in Fig. 1 as an example to indicate the purity of data sample used for Dalitz plot analysis in the LHCb experiment.

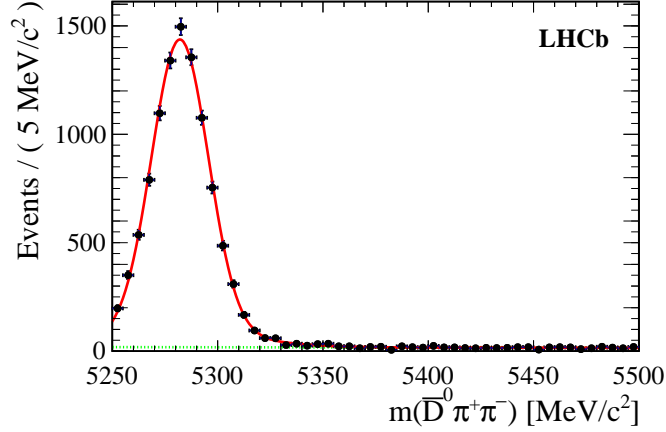


Figure 1: Invariant mass distribution of $B^0 \rightarrow \bar{D}^0 \pi^+ \pi^-$ candidates. Data points are shown in black. The fit is shown as a solid (red) line with the background component displayed as dashed (green) line.

3. Excited $D_{(s)}$ spectroscopy

The $D_{(s)}$ system includes a heavy charm quark and a light satellite quark. In the heavy quark limits, the two parts can be decoupled. The spin of the charm quark is $1/2$, $D_{(s)}$ states thus appear in doublet with similar widths, but one with natural spin-parity (0^+ , 1^- , 2^+ , ...) and the other with unnatural spin-parity (0^- , 1^+ , 2^- , ...). Dalitz plot analyses discussed in these proceedings only contain information about excited $D_{(s)}$ mesons with natural spin-parity.

Inclusive studies on $D_{(s)}$ spectroscopy have been performed previously by both the LHCb experiment [8, 9] and the Babar experiment [10]. Excited states of $D^*(2650)$, $D^*(2760)$ and $D^*(3000)$ with natural spin-parity have been observed for D^* spectrum. Similarly, excited states of $D_s^*(2700)$, $D_s^*(2860)$ and $D_s^*(3040)$ with natural spin-parity have been observed for D_s^* spectrum. These new excited states have not been confirmed by any other experiments and their spins are not determined.

The large amount of exclusive decay samples of $B \rightarrow Dhh$ decays are ideal places for the study of these newly observed states. Indeed, a D^{*+} resonance with spin 3 and mass around $2.79 \text{ GeV}/c^2$ has been observed in the Dalitz plot analysis of the $B^0 \rightarrow \bar{D}^0 \pi^+ \pi^-$ decay and a D^{*0} resonance with spin 1 and mass also around $2.79 \text{ GeV}/c^2$ has been observed in the Dalitz plot analysis of the $B^- \rightarrow D^+ K^- \pi^-$ decay. In the Dalitz plot analysis of the $B_s^0 \rightarrow \bar{D}^0 K^- \pi^+$ decay, a mixture of spin-1 and spin-3 D_s^* resonances has been found in mass around $2.86 \text{ GeV}/c^2$. The spin assignments of the $D_{(s)}$ excited states are determined using hypothesis test by assuming different spin hypotheses. The measured masses and widths of these newly observed excited states are summarised in Table 1. The observed states are consistent with the predictions of D -wave excited states.

4. Light meson structure

Significant contributions from both $B^0 \rightarrow \bar{D}^0 f_0(500)$ and $B^0 \rightarrow \bar{D}^0 f_0(980)$ decays are observed in the Dalitz plot analysis of $B^0 \rightarrow \bar{D}^0 \pi^+ \pi^-$ and can be used to obtain information on the substructure of the $f_0(980)$ and $f_0(500)$ resonances within the factorisation approximation. Two models for the quark structure of those states are considered: $q\bar{q}$ or $[qq'][\bar{q}\bar{q}']$ (tetraquarks). In both models,

Table 1: Summary of measured masses and widths of newly observed excited $D_{(s)}$ states. The mass and width of $D_3^{*+}(2760)$ are presented in the two models used for the Dalitz plot analysis.

$D_{(s)}^*$	mass (MeV)	width (MeV)
$D_3^{*+}(2760)$ (isobar)	$2798 \pm 7 \pm 1 \pm 7$	$105 \pm 18 \pm 6 \pm 23$
$D_3^{*+}(2760)$ (K-matrix)	$2802 \pm 11 \pm 10 \pm 3$	$154 \pm 27 \pm 13 \pm 9$
$D_1^{*0}(2760)$	$2791 \pm 18 \pm 11 \pm 6$	$177 \pm 32 \pm 20 \pm 7$
$D_{s1}^*(2860)$	$2859 \pm 12 \pm 6 \pm 23$	$159 \pm 23 \pm 27 \pm 72$
$D_{s3}^*(2860)$	$2860.5 \pm 2.6 \pm 2.5 \pm 6.0$	$53 \pm 7 \pm 4 \pm 6$

mixing angles between different quark states are determined using our measurements. In the $q\bar{q}$ model, the mixing between $s\bar{s}$ and $u\bar{u}$ or $d\bar{d}$ can be written as

$$|f_0(980)\rangle = \cos \varphi_{\text{mix}} |s\bar{s}\rangle + \sin \varphi_{\text{mix}} |n\bar{n}\rangle, \quad (4.1)$$

$$|f_0(500)\rangle = -\sin \varphi_{\text{mix}} |s\bar{s}\rangle + \cos \varphi_{\text{mix}} |n\bar{n}\rangle, \quad (4.2)$$

where $|n\bar{n}\rangle \equiv (|u\bar{u}\rangle + |d\bar{d}\rangle)/\sqrt{2}$ and φ_{mix} is the mixing angle. In the $[qq'][\bar{q}\bar{q}']$ model, the mixing angle, ω_{mix} , is introduced and the mixing becomes

$$|f_0(980)\rangle = \cos \omega_{\text{mix}} |n\bar{n}s\bar{s}\rangle + \sin \omega_{\text{mix}} |u\bar{u}d\bar{d}\rangle, \quad (4.3)$$

$$|f_0(500)\rangle = -\sin \omega_{\text{mix}} |n\bar{n}s\bar{s}\rangle + \cos \omega_{\text{mix}} |u\bar{u}d\bar{d}\rangle. \quad (4.4)$$

In both cases, the following experimentally measured variable is defined

$$r^f = \frac{Br(B^0 \rightarrow \bar{D}^0 f_0(980))}{Br(B^0 \rightarrow \bar{D}^0 f_0(500))} \times \frac{\Phi(500)}{\Phi(980)}, \quad (4.5)$$

where $\Phi(500)$ and $\Phi(980)$ are the integrals of the phase-space factors. The parameter r^f is related to the mixing angle by the equation

$$r^f = \tan^2 \varphi_{\text{mix}} \times \left| \frac{F(B^0 \rightarrow f_0(980))}{F(B^0 \rightarrow f_0(500))} \right|^2 \quad (4.6)$$

in the $q\bar{q}$ model and by

$$r^f = \left| \frac{1 - \sqrt{2} \tan \omega_{\text{mix}}}{\tan \omega_{\text{mix}} + \sqrt{2}} \right|^2 \times \left| \frac{F(B^0 \rightarrow f_0(980))}{F(B^0 \rightarrow f_0(500))} \right|^2 \quad (4.7)$$

in the $[qq'][\bar{q}\bar{q}']$ tetraquark model. The form factors $F(B^0 \rightarrow f_0(980))$ and $F(B^0 \rightarrow f_0(500))$ are evaluated at the four-momentum transfer squared equal to the square of the \bar{D}^0 mass. Values of the mixing angles as a function of form factor ratio are obtained in Fig. 2 for the $q\bar{q}$ model and the $[qq'][\bar{q}\bar{q}']$ tetraquark model using measured value of $r^f = 0.177_{-0.062}^{+0.066}$.

The ratio of form factors is expected to be close to unity. However, the limit set on the branching fraction measurement of $B_s^0 \rightarrow \bar{D}^0 f_0(980)$ [13] is below the value expected in a simple model based on our measured value of $Br(B^0 \rightarrow \bar{D}^0 f_0(500))$ and assuming equal form factors. More complicated models may be needed in order to explain all results.

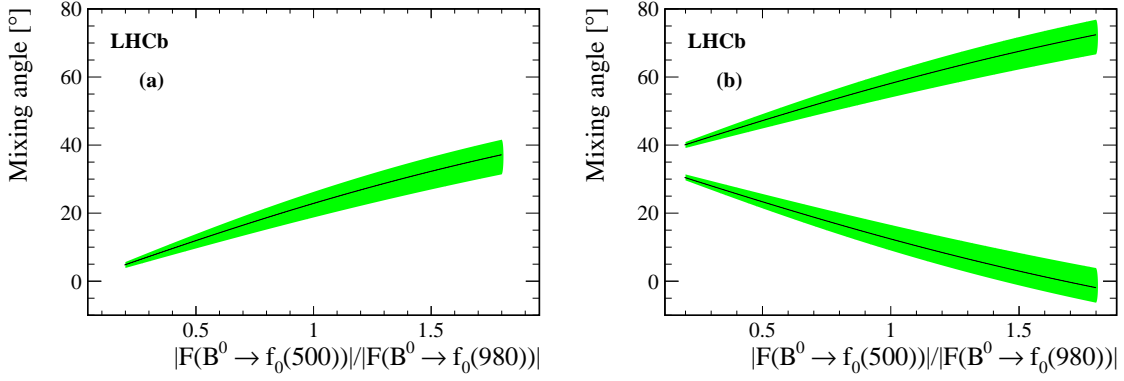


Figure 2: Mixing angle as a function of form factor ratio for the (a) $q\bar{q}$ model and (b) $[qq'][\bar{q}\bar{q}']$ tetraquark model. Green band gives 1σ interval around central values (black solid line).

Table 2: Results of $R_{D\rho}$ and $\cos \delta_{D\rho}$.

Model	$R_{D\rho}$	$\cos \delta_{D\rho}$
Isobar	0.69 ± 0.15	$0.984^{+0.113}_{-0.048}$
K-matrix	0.69 ± 0.15	$0.987^{+0.114}_{-0.048}$

5. Isospin analysis of the $B \rightarrow D\rho$ system

The measured branching fraction of the $B^0 \rightarrow \bar{D}^0 \rho(770)^0$ decay is used to perform an isospin analysis, together with those of the $B^+ \rightarrow \bar{D}^0 \rho(770)^+$, $B^0 \rightarrow D^- \rho(770)^+$ decays. The amplitudes of the decays can be written as linear combinations of the isospin eigenstates A_I with $I = 1/2$ and $3/2$ [14, 15] assuming isospin symmetry

$$\begin{aligned}
 A(\bar{D}^0 \rho^+) &= \sqrt{3}A_{3/2}, \\
 A(D^- \rho^+) &= \sqrt{1/3}A_{3/2} + \sqrt{2/3}A_{1/2}, \\
 A(\bar{D}^0 \rho^0) &= \sqrt{2/3}A_{3/2} - \sqrt{1/3}A_{1/2},
 \end{aligned} \tag{5.1}$$

In the heavy-quark limit, the factorisation model predicts [16, 17] $\delta_{D\rho}$, the strong phase difference between the amplitudes $A_{1/2}$ and $A_{3/2}$, to be $\mathcal{O}(\Lambda_{\text{QCD}}/m_b)$ and the amplitude ratio, $R_{D\rho} \equiv \frac{|A_{1/2}|}{\sqrt{2}|A_{3/2}|}$, to be $1 + \mathcal{O}(\Lambda_{\text{QCD}}/m_b)$, where m_b represents the b quark mass and Λ_{QCD} the QCD scale.

Using our measurement of $Br(B^0 \rightarrow \bar{D}^0 \rho^0)$, the world average values of $Br(B^0 \rightarrow D^- \rho^+)$, $Br(B^+ \rightarrow \bar{D}^0 \rho^+)$, and the ratio of lifetimes $\tau(B^+)/\tau(B^0)$ [18], $R_{D\rho}$ and $\cos \delta_{D\rho}$ are calculated for the isobar and K-matrix models used for the Dalitz plot analysis of the $B^0 \rightarrow \bar{D}^0 \pi^+ \pi^-$ decay and summarised in Table 2. These results are not significantly different from the predictions of factorisation models. Non-factorisable final-state interaction effects do not introduce a sizeable phase difference between the isospin amplitudes in the $B \rightarrow D\rho$ system. The precision on $R_{D\rho}$ and $\cos \delta_{D\rho}$ is dominated by that of the branching fractions of the decays $B^+ \rightarrow \bar{D}^0 \rho(770)^+$ and $B^0 \rightarrow D^- \rho(770)^+$.

6. Conclusion

Decays of b -hadrons to three-body final states including an open-charmed meson provide rich physics results using Dalitz plot analysis technique. The LHCb experiment has performed Dalitz plot analyses for the $B^0 \rightarrow \bar{D}^0 \pi^+ \pi^-$, $B^0 \rightarrow \bar{D}^0 K^+ \pi^-$, $B^- \rightarrow D^+ K^- \pi^-$ and $B_s^0 \rightarrow \bar{D}^0 K^- \pi^+$ decays. Using B^0/B^+ decays, a spin-1 D^{*0} meson and a spin-3 D^{*+} meson have been observed at mass around $2.79 \text{ GeV}/c^2$. Similarly, a spin-1 and a spin-3 D_s^* mesons have been observed at mass around $2.86 \text{ GeV}/c^2$ in the B_s^0 decay. Studies have also been performed to constrain the mixing angle between the $f_0(500)$ and $f_0(980)$ resonances using the measured branching fraction of the $B^0 \rightarrow \bar{D}^0 f_0(980)$ and $B^0 \rightarrow \bar{D}^0 f_0(500)$ decays. An isospin analysis in the $B \rightarrow D\rho$ decays using our improved measurement of the branching fraction of the decay $B^0 \rightarrow \bar{D}^0 \rho^0$ is performed, indicating that non-factorisable effects from final-state interactions are limited in the $D\rho$ system.

The Dalitz plot analyses shown in the proceedings are performed using the Cabbibo-favored decay $D^0 \rightarrow K^- \pi^+$ and the CP violation effect is negligible. With D^0 decaying to CP eigenstates, (time-dependent) Dalitz plot measurement could be performed and will give sensitivities to the CKM angles using the current LHCb data.

References

- [1] T. Gershon, On the measurement of the unitarity triangle angle γ from $B^0 \rightarrow DK^*$ decays, Phys. Rev. D79 (2009) 051301, arXiv:0810.2706; T. Gershon and M. Williams, Prospects for the measurement of the unitarity triangle angle γ from $B^0 \rightarrow DK^+ \pi^-$ decays, Phys. Rev. D80 (2009) 092002, arXiv:0909.1495.
- [2] S. Nandi and D. London, $B_s(\bar{B}_s) \rightarrow D_{CP}^0 K \bar{K}$: Detecting and discriminating new physics in B_s - \bar{B}_s mixing, Phys. Rev. D85 (2012) 114015, arXiv:1108.5769; T. Latham and T. Gershon, A method to measure $\cos(2\beta)$ using time-dependent Dalitz plot analysis of $B^0 \rightarrow D_{CP} \pi^+ \pi^-$, J. Phys. G36 (2009) 025006, arXiv:0809.0872 [hep-ph]; J. Charles, A. Le Yaouanc, L. Oliver, O. Pene and J. C. Raynal, $B_d^0(t) \rightarrow DPP$ time-dependent Dalitz plots, CP-violating angles 2β , $2\beta + \gamma$, and discrete ambiguities, Phys. Lett. B425 (1998) 375, arXiv:hep-ph/9801363.
- [3] W. Wang and C.-D. Lu, Distinguishing two kinds of scalar mesons from heavy meson decays, Phys. Rev. D82 (2010) 034016, arXiv:0910.0613; J.-W. Li, D.-S. Du, and C.-D. Lu, Determination of f_0 - σ mixing angle through $B_s^0 \rightarrow J/\psi f_0(980)(\sigma)$ decays, Eur. Phys. J. C72 (2012) 2229, arXiv:1212.5987 and references therein.
- [4] LHCb collaboration, R. Aaij et al., Dalitz plot analysis of $B^0 \rightarrow \bar{D}^0 \pi^+ \pi^-$ decays, Phys. Rev. D92 (2015) 032002, arXiv:1505.01710.
- [5] LHCb collaboration, R. Aaij et al., Amplitude analysis of $B^0 \rightarrow \bar{D}^0 K^+ \pi^-$ decays, Phys. Rev. D92 (2015) 012012, arXiv:1505.01505.
- [6] LHCb collaboration, R. Aaij et al., First observation and amplitude analysis of the $B^- \rightarrow D^+ K^- \pi^-$ decays, Phys. Rev. D91 (2015) 092002, arXiv:1503.02995.
- [7] LHCb collaboration, R. Aaij et al., Dalitz plot analysis of $B_s^0 \rightarrow \bar{D}^0 K^- \pi^+$ decays, Phys. Rev. D90 (2014) 072003, arXiv:1407.7712; LHCb collaboration, R. Aaij et al., Observation of overlapping spin-1 and spin-3 $\bar{D}^0 K^-$ resonances at mass $2.86 \text{ GeV}/c^2$, Phys. Rev. Lett. 113 (2014) 162001.
- [8] LHCb collaboration, R. Aaij et al., Study of D_J meson decays to $D^+ \pi^-$, $D^0 \pi^+$, $D^{*+} \pi^-$ final states in pp collision, JHEP 09 (2013) 145, arXiv: 1307.4556.

- [9] LHCb collaboration, R. Aaij et al., Study of D_{sJ} decays to D^+K_s and D^0K^+ final states in pp collisions, JHEP 10 (2012) 151, arXiv:1207.6016.
- [10] Babar collaboration, B. Aubert et al., Study of D_{sJ} decays to D^*K in inclusive e^+e^- interactions, Phys. Rev. D80 (2009) 092003, arXiv:0908.0806.
- [11] BaBar collaboration, B. Aubert et al., Dalitz plot analysis of the decay $B^\pm \rightarrow K^\pm K^\pm K^\mp$, Phys. Rev. D74 (2006) 032003, arXiv:hep-ex/0605003.
- [12] BES collaboration, M. Ablikim et al., Evidence for $f_0(980)$ production in χ_{c0} decays, Phys. Rev. D70 (2004) 092002, arXiv:hep-ex/0406079.
- [13] LHCb collaboration, R. Aaij et al., Search for the decay $B_s^0 \rightarrow D^0 f_0(980)$, JHEP 08 (2015) 005, arXiv:1505.01654.
- [14] M. Neubert and A. A. Petrov, Comments on color-suppressed hadronic B decays, Phys. Lett. B519 (2001) 50, arXiv:hep-ph/0108103.
- [15] J. L. Rosner, Large final state phases in heavy meson decays, Phys. Rev. D60 (1999) 074029, arXiv:hep-ph/9903543.
- [16] M. Beneke, G. Buchalla, M. Neubert, and C. T. Sachrajda, QCD factorization for exclusive, nonleptonic B meson decays: general arguments and the case of heavy-light final states, Nucl. Phys. B591 (2000) 313, arXiv:hep-ph/0006124.
- [17] H.-Y. Cheng and K.-C. Yang, Updated analysis of a_1 and a_2 in hadronic two-body decays of B mesons, Phys. Rev. D59 (1999) 092004, arXiv:hep-ph/9811249.
- [18] Particle Data Group, K. A. Olive et al., Review of particle physics, Chin. Phys. C38 (2014) 090001.